# Molecular Dynamics Simulations of Normal Mode Vibrational Energy Transfer in Liquid Nitromethane

**Vinayak N. Kabadi**

*Chemical Engineering Department, North Carolina A&T State University, Greensboro, North Carolina 27411*

**Betsy M. Rice***

*U.S. Army Research Laboratory, Aberdeen Proving Ground, Maryland 21005*

*Received: July 9, 2003; In Final Form: November 12, 2003*

Nonequilibrium molecular dynamics simulations are used to study vibrational energy relaxation (VER) in liquid nitromethane after excitation of the C−H stretching vibrations. The simulated liquid consists of a mixture of excited and unexcited molecules, where the unexcited molecules were used to monitor excitation of the bath upon vibrational relaxation of the excited molecules. A previously developed projection method (Raff, L. M. *J. Chem. Phys*. **1988**, *89*, 5680) was employed to monitor the normal-mode kinetic energies of vibrations in both excited and unexcited molecules as functions of time. Overall, the results are in qualitative agreement with experimental measurements of VER in liquid nitromethane after mid-IR excitation in the C−H stretching region (Deak, J. C., Iwaki, L. K., Dlott, D. D. *J. Phys. Chem. A* **1999**, *103*, 971). The simulation results indicate that the excited C−H stretching vibrations deposit energy predominantly into the remaining vibrations in the molecules. These vibrations relax at different rates, resulting in a multistage vibrational cooling process for nitromethane, in agreement with experimental results. The excitation of vibrations of the surrounding unexcited molecules occurs through indirect rather than direct intermolecular vibrational energy transfer processes, also in agreement with experiment.

## I. Introduction

Attaining an elemental understanding of the conversion of condensed-phase energetic materials to final products is a formidable endeavor since the overall process consists of several complex, concerted chemical and physical events and depends strongly on the conditions of initiation. For example, a sufficiently strong shock can initiate the detonation of an energetic material, a process that can be thought of as a reaction wave that proceeds through a material at supersonic speeds. Direct measurements of mechanistic details that would provide a fundamental description of the initiation process leading to detonation are lacking due to substantial experimental obstacles. Thus, a definitive description of the process is not available. However, the chemically interesting behavior of these materials has inspired numerous researchers to propose theories to explain shock initiation to detonation. One leading theory that has enjoyed substantial experimental exploration suggests multiphonon up pumping has a prominent role in shock initiation of energetic materials.[1−9]

This process begins with the heating of the phonons of a material upon the passage of a shock wave, where "phonon" refers to the continuum of low-frequency lattice vibrations in a solid or the instantaneous normal modes of a liquid.[9] The excess energy of the phonons flows into the cold molecular modes of the material through "doorway vibrations"[9] of the molecules. Doorway vibrations are low-frequency modes that are strongly coupled to the phonon bath and whose frequencies are near that of the maximum frequency of the phonon continuum.[9] As energy continues to flow from the overheated phonon bath into the doorway vibrations, higher energy vibrational modes are subsequently excited through intramolecular vibrational energy transfer. This "up pumping" of vibrational states continues until sufficient energy is localized in the reaction coordinates of the molecules to allow reactions. Dlott and co-workers have performed extensive experimental investigations of energy transfer in condensed-phase molecular systems to assess various aspects of this theory.[9−15] These include increasingly detailed spectroscopic studies designed to extract mechanistic details of vibrational energy relaxation (VER),[12] the dissipation of excess energy from vibrations excited by a pump pulse to other vibrations in the molecule or to the phonon bath; vibrational cooling (VC),[12] the complete loss of excess energy of the vibrationally excited molecule to the surrounding medium; and intermolecular vibrational energy transfer (IVET),[11] the process of vibrational energy transfer from one molecule to another in the bath either through direct or indirect processes. A direct IVET process is one in which energy is transferred from a specific vibration of one molecule directly to a vibration in another molecule. Indirect IVET refers to a two-step process in which VC of the excited molecule first results in the heating of the bath. Subsequently, the bath transfers its excess energy to vibrational states of other molecules in the bath through multiphonon up pumping.[11] Dlott and co-workers have performed a series of spectroscopic studies of VER in liquid nitromethane (NM) that have demonstrated that the VER process in this system is fairly complex.[9−12] The most recent study[12] used anti-Stokes Raman spectroscopy to measure instantaneous vibrational populations of NM after infrared excitation in the C−H stretching region (near 2970 $cm^{-1}$) for the neat liquid. Deak et al. report that this pulse excites the C−H stretching vibrations and the first overtones of the antisymmetric $CH_3$ bending and $NO_2$ stretching vibrations.[12] Additionally, Deak et

* To whom correspondence should be addressed.

10.1021/jp035975v CCC: $27.50 
Published on Web 01/03/2004

al. applied this IR−Raman method to solutions of NM-$CCl_4$ to extract details of energy flow that could not be obtained from experiments on the neat liquid. Since $CCl_4$ is transparent at 2970 $cm^{-1}$, it was used as a "molecular thermometer" to monitor the excitation of the bath upon VC of NM.[12] Monitoring the populations of $CCl_4$ vibrations after pump pulse excitation of the NM provided insight into the mechanism of VC for NM. The data show that the relaxation takes place in three steps. First, energy deposited in the C−H stretch (and in the first overtones of the antisymmetric $NO_2$ stretching and CH bending vibrations) is redistributed to all other vibrations within a few picoseconds. The NM-$CCl_4$ results do not reflect excitation of the $CCl_4$ during this time, indicating that the initial VER is intramolecular. Subsequently, the higher energy vibrations of NM (1560 and ∼1400 $cm^{-1}$) relax on the time scale of ∼15 ps, mainly by populating the lower energy vibrations (all transitions below ∼1400 $cm^{-1}$). The NM-$CCl_4$ results show that approximately one-third of the energy from the decay of these two transitions is dissipated to the bath. Finally, the lower energy vibrations excited in the first two stages relax by heating the bath. VC of NM occurs on the 50−100 ps time scale, with the response of the $CCl_4$ vibrational transitions after excitation of the NM rising on the same time scale. This indicates that the excitation of the bath molecules occurs mainly through indirect IVET processes.

While these experimental studies have produced detailed data leading to a basic understanding of underlying processes that could affect or control shock initiation to detonation of NM, they could benefit from complementary theoretical studies. Such studies could be used to interpret complicated spectra, follow growth and loss of energies in vibrational modes whose transitions cannot currently be resolved using available experimental techniques, or explore VER processes under conditions not amenable to measurement. Since the theory of up pumping to initiation of detonation is based on mechanisms of energy flow within a shocked system, it is imperative that energy transfer in the explosive be well characterized. In an effort to contribute to the achievement of this characterization, we will explore the vibrational excitation and relaxation in liquid NM using classical molecular dynamics (MD) computer simulations.

Nitromethane has been a popular system for use in theoretical studies of energetic materials due to its relatively small size and availability of extensive experimental data in all phases, against which comparisons can be made. In addition to numerous quantum mechanical characterizations,[16−26] nitromethane has been subjected to molecular dynamics simulations using a variety of models.[27−39] The gas-phase simulations focused on unimolecular reactions.[27] With the exception of two MD simulations in which the forces were evaluated "on the fly" using DFT,[30,39] the condensed-phase MD simulations have been used to study nonreactive processes and evaluate thermodynamic properties at a variety of temperatures and pressures.[28−38] To our knowledge, there have been no theoretical studies that have explored transfer of energy through vibrational modes of nitromethane molecules or from molecular modes to phonon states.

There have been numerous theoretical studies to explore vibrational energy relaxation in liquids.[40−67] Unfortunately, a rigorous QM treatment of this problem is beyond available computational resources; any such treatment could only be applied to systems with a limited number of degrees of freedom. The approaches employed to study VER in liquids range from mixed quantum classical[40−57] to fully classical studies using either equilibrium or nonequilibrium molecular dynamics (NEMD).[58−67] A popular semiclassical method treats the vibrational modes of a single solute molecule quantum mechanically and the remaining degrees of freedom in the liquid classically. State-to-state rate constants are then evaluated with perturbative approaches using time-correlation functions (TCFs) of the generalized forces of the bath acting on the vibrational modes of the solute.[40−49] A sample of recent VER studies using this approach has been carried out for several systems, including $D_2O$, $CH_3Cl$, $N_2$, and $O_2$.[44−49] While these studies have given insight into VER mechanisms in the liquid state, applications using these methods are limited to processes for which the perturbative approaches do not break down. Further, they require quantum correction factors to the classical TCFs[68] and have only been applied to systems wherein the quantum particle has only a few vibrational degrees of freedom. Additionally, they are also influenced by the description of the intermolecular interactions in the classical fluid (as in any purely classical MD simulation) and often the solvent molecules are assumed to be rigid or have reduced dimensionality. Other approaches have been developed to overcome the limitations of the standard perturbative approaches;[50−57] however, they also appear to be very computationally expensive and have been applied to very small systems.

Limitations of purely classical MD simulations for VER include neglect of zero-point energy, an inability to describe other quantum processes, and reliance on the descriptions of interatomic interactions (as for the semiclassical models described above). However, this approach requires modest computational resources even for large numbers of molecules, lengthy simulations, or complex descriptions of the interatomic interactions. Also, classical MD simulations often provide results that are in agreement with experimental measurements.[36−38] Additionally, classical MD can be used to simulate nonequilibrium processes[58−67,69−75] such as the VC of highly excited molecules and multiphonon up pumping of the bath molecules as in the Deak et al. experiments.[12] Therefore, we have chosen the method of classical nonequilibrium molecular dynamics to study vibrational energy transfer in NM.

The NEMD method we will implement to study VER in NM follows an approach developed by Raff[69] and used in several NEMD studies of VER and reaction dynamics.[69−73] In these simulations, energy flow from an excited vibrational mode to other modes within a molecule is monitored by a method in which instantaneous Cartesian velocities are projected onto the normal-mode eigenvectors during the trajectory integration. Implementation of the Raff approach to the problem presented here is appealing mainly because of its ease of implementation using standard classical molecular simulation techniques and because it provides a temporal description of energy flow among the individual vibrational modes of the system. We felt that the application of this method would allow for a direct comparison of simulation results with those of the Deak et al. experiments,[12] in which specific vibrational modes are excited and energy flow among the various degrees of freedom was monitored. In particular, we will use classical NEMD simulations to study the energy transfer in liquid NM after excitation of the C−H stretching vibrations.

## II. Model and MD Simulations Procedure

**A. Potential Energy Function.** The function used to describe intermolecular interactions for liquid nitromethane was previously developed and assessed in a series of molecular simulations of NM in the condensed phase.[36−38] Intramolecular terms to represent stretching, bending, and torsional motions within

**TABLE 1: Nitromethane Vibrations**

| | | | frequencies, $cm^{-1}$ | | |
|---|---|---|---|---|---|
| mode | assignment | description | Deak et al.[a] | this work | B3LYP/ 6-31G* [b] |
| $\nu_1$ | $\nu_a(CH_3)$ | $CH_3$ asym stretch | 3050 | 3095 | 3100 (1.00) |
| $\nu_2$ | $\nu_a(CH_3)$ | $CH_3$ asym stretch | 3050 | 3093 | 3070 (1.00) |
| $\nu_3$ | $\nu_s(CH_3)$ | $CH_3$ sym stretch | 2968 | 2961 | 2981 (0.98) |
| $\nu_4$ | $\nu_a(NO_2)$ | $NO_2$ asym stretch | 1560 | 1618 | 1615 (1.00) |
| $\nu_5$ | $\delta_a(CH_3)$ | $CH_3$ asym bend | 1426 | 1436 | 1444 (0.99) |
| $\nu_6$ | $\delta_a(CH_3)$ | $CH_3$ asym bend | 1426 | 1434 | 1432 (1.00) |
| $\nu_7$ | $\delta_s(CH_3)$ | $CH_3$ sym bend | 1402 | 1508 | 1364 (0.95) |
| $\nu_8$ | $\nu_s(NO_2)$ | $NO_2$ sym stretch | 1379 | 1368 | 1388 (0.96) |
| $\nu_9$ | $\rho(CH_3)$ | $CH_3$ rock | 1125 | 1101 | 1101 (0.99) |
| $\nu_{10}$ | $\rho(CH_3)$ | $CH_3$ rock | 1104 | 1053 | 1076 (0.99) |
| $\nu_{11}$ | $\nu_s(CN)$ | CN sym stretch | 918 | 821 | 892 (0.92) |
| $\nu_{12}$ | $\delta_s(NO_2)$ | $NO_2$ sym bend | 657 | 605 | 636 (0.92) |
| $\nu_{13}$ | $\rho(NO_2)$ | $NO_2$ rock | 607 | 601 | 584 (0.94) |
| $\nu_{14}$ | $\rho(NO_2)$ | $NO_2$ rock | 480 | 461 | 461 (0.99) |
| $\nu_{15}$ | $\tau(CH_3)$ | methyl rotation | 60 | 117 | 51 (0.94) |

[a] Reference 12. [b] Reference 36. Values in parentheses denote the projection of the model's eigenvectors onto the B3LYP/6-31G* eigenvectors. A value of 1 indicates that the eigenvectors are in exact agreement.

each molecule are also included, with a full description and parameters given in ref 38. The NM frequencies using this model, their approximate assignments, and projection of the corresponding eigenvectors onto the ab initio information to which the model was fitted and are given in Table 1. Also, measured NM frequencies reported by Deak et al.[12] are given in this table. Normal mode vibrational frequencies and eigenvectors calculated using this model are in overall good agreement with the quantum mechanical results. The largest disagreement in the model and the ab initio frequencies are for the $CH_3$ symmetric bend; the model predicts a frequency that is $\sim$140 $cm^{-1}$ larger than the B3LYP result and $\sim$100 $cm^{-1}$ larger than the experimental value. The projections of the eigenvectors for this model onto the ab initio eigenvectors indicates that the descriptions of the atomic motions for the molecular vibrations are good in the neighborhood of the potential energy minimum.

**B. Simulation Details.** All MD simulations were carried out using the DLPOLY2.0 set of codes.[76] All simulations used a cubic cell containing 480 NM molecules. Periodic boundary conditions were imposed in all dimensions and a cutoff distance of 15 Å was used for the calculation of interatomic forces. Standard long-range corrections for the energy and virial contributions were included. The Coulombic long-range interactions were handled using Ewald's method.[77] A time step of 0.5 fs was used in all the simulations.

Simulations under conditions of constant temperature and pressure should provide a better chance for comparison of the simulation results with the experimental data of Deak et al.[12] However, the modified equations of motion used to perform NPT-MD simulations, such as those introduced by Berendsen[78] or the Melchionna modification of the Hoover-Nose equations,[79] couple each atomic velocity with a barostat and thermostat in order to drive the system to the desired thermodynamic state. Therefore, energy flow is affected through integration of the isothermal−isobaric equations of motion. To circumvent this, we performed constant energy constant volume (NVE) MD simulations to monitor energy among the various degrees of freedom.

**C. Projection Method to Evaluate Instantaneous Normal Modes.** In an attempt to simulate the Deak et al. experiments[12] using classical MD, we utilized the projection methods developed by Raff[69] to follow the energy flow from excited molecular vibrational modes. Energy flow among vibrational normal modes of a molecule can be monitored during a trajectory by projecting instantaneous Cartesian velocities onto normal mode eigenvectors and calculating the individual normal mode kinetic energies. Details of the method are given in ref 69. The method and its application in this work is analogous to applications by Raff,[69−73] with the only significant difference being that we have applied the method to molecules in the liquid state. This method has the advantage of allowing a direct comparison of MD simulation results with the temporal profiles of anti-Stoke transients from NM after pump pulse excitation of various vibrational modes.

The correct application of this method in this study requires that before the projection of the atomic velocities for each molecule is performed, its Cartesian frame must be translated and rotated such that it coincides with that of the molecular structure that was used to generate the eigenvectors onto which the velocities will be projected. This structure will be referred to as the "reference structure". The atomic arrangement of the reference structure is such that the nitrogen atom is located at (0,0,0) and the C atom is located on the $-z$-axis. Therefore, the C−N bond of the molecule lies along the $z$-axis. The heavy atoms of the reference structure all fall in the $x-z$ plane. This choice of reference frame is not unique.

The Cartesian frame of each molecule in the MD simulation cell will be referred to hereafter as the "lab-fixed Cartesian frame". This frame can be superimposed onto that of the reference structure by the following procedure:

1. Shift the coordinates of the molecule so that the origin is located on the nitrogen atom.

2. Rotate the molecule about the origin such that the vector defining the C−N bond is aligned with the $z$-axis, and C located on the $-z$-axis.

3. Finally, rotate the molecule about the $z$-axis such that the vector defining one of the N−O bonds lies in the $x-z$ plane and the two oxygen atoms are in the same quadrants as their counterparts in the reference structure. Thus, while the four heavy atoms in the reference structure all fall on the $x-z$ plane, this step requires that C, N, and only one of the O atoms be coplanar.

4. Since the Cartesian frames of the molecule and reference structure are now coincident, the atomic velocities can be projected onto the normal mode eigenvectors, and the instantaneous normal mode kinetic energies can be calculated.

The projection method is applied in two ways in this study: The first application is used in the initial condition selection to excite certain vibrational modes. The method is also used to monitor the energy flow to and from the vibrational modes of the molecules within the system.

**D. Initial Condition Selection.** To generate a fully equilibrated liquid at the conditions of the experiment before excitation, an NPT MD simulation at 294 K, 1 atm was performed. The resulting average density of the liquid is 1.090 $g/cm^3$, which is somewhat lower than the experimental value[80] of 1.137 $g/cm^3$ at 293 K. It is, however, close to the previous simulation results[37] of 1.103 $g/cm^3$ at 290 K and 1.093 $g/cm^3$ at 298 K, in which a slightly different intramolecular force field was used.

Next, an NVE-MD simulation of liquid NM assuming a density of 1.090 $g/cm^3$ was performed for 800 000 steps, of which the first 100 000 steps were equilibration. During the equilibration period, atomic velocities were scaled every fifth step in order to achieve the desired temperature (294 K). After

equilibration, the trajectory integration continued without scaling the atomic velocities. A configuration file containing atomic positions and velocities was created at the 150 000th step after equilibration; 11 other configuration files were generated at subsequent 50 000 step-intervals. The atomic positions and velocities within these files were used to generate the initial conditions for 12 NEMD simulations of energy flow from excited CH stretching modes.

To complete the initial condition selection for the simulations designed to monitor energy flow, a percentage of the molecules in the equilibrated liquid were selected for mode-specific excitation. We did not identify information in the experimental papers that would allow us to quantify the populations of the various vibrational states that are excited from the mid-IR pulse. Deak et al.[12] report that mainly the $\nu_3$ symmetric C−H stretch is populated, but the antisymmetric C−H stretching modes are also excited ($\nu_1$ and $\nu_2$). Also, monitoring the anti-Stokes transients during the experiment led Deak et al. to conclude the $NO_2$ stretching fundamentals and first overtones of the antisymmetric $CH_3$ bending vibrations are excited by the pump pulse. Since we did not have quantitative information on vibrational populations, we arbitrarily chose the percentage of molecules that would be excited and the manner of distribution of excitation energy in the specified vibrational modes. We chose to excite 25% of the molecules, with the excitation energy equipartitioned among the three CH stretching vibrations.

From each of the configuration files, 120 molecules were randomly selected for excitation. The lab-fixed Cartesian frame for each of the 120 molecules was then translated and rotated as described in section II.C to coincide with that of the reference structure, thus allowing for a proper description of normal mode velocities. The kinetic energy for each of the CH symmetric and asymmetric stretching modes of all 120 molecules was increased by 0.692 kcal/mol through appropriate scaling of the normal coordinate velocities corresponding to these modes. Thus, an excess energy of 249.05 kcal/mol was introduced into the system, which would result in an expected temperature rise of 12.4 K, a value that is close to the experimental temperature jump resulting from the pump pulses in neat NM (∼10 K).[12] The atomic velocities were then transformed back to the lab-fixed Cartesian frame, thus providing the initial conditions for the NVE MD simulation to study the redistribution of the excitation energy. The duration of each NVE MD simulation is 60 ps.

A few simulations were performed to explore the dependence of energy transfer upon the concentration of excited molecules. In a set of 10 trajectories, only one molecule was excited out of a total of 240 molecules and monitored. The fluctuations in the normal mode kinetic energies of these excited molecules were extreme and resulting statistics from averaging over these 10 trajectories were extremely poor. To obtain a reasonable statistical result, it would be necessary to perform an extremely large number of these simulations; the computational cost was deemed prohibitive. Therefore, we chose to excite a larger number of molecules in the liquid for this study.

The dependence of the energy transfer upon the level of excitation when 25% of the molecules are excited was also explored. We found that exciting the molecules to energies 3 times larger than those used in our production runs did not change the mechanism of energy transfer to the unexcited molecules.

**E. Trajectory Analysis.** Atomic positions and velocities were recorded at intervals of every 100 time steps during integration of each of the 12 NEMD simulations described in section II.D.

**TABLE 2: Properties of Liquid Nitromethane before Excitation and after Excitation from NVE Simulations**

| | before excitation | after excitation[a] | difference[b] |
|---|---|---|---|
| $T$, K | 293.5 ± 0.0 | 306.1 ± 0.2 | |
| $\rho$, g/cm$^3$ | 1.090 | 1.090 | |
| $P$, bar | 1.0 ± 0.1 | 102 ± 40 | |
| $E_{total}$,[c] kcal/mol | 1.068 ± 0.000 | 1.587 ± 0.001 | 0.519 ± 0.001 |
| $E_{kinetic}$,[c] kcal/mol | 6.124 ± 0.000 | 6.387 ± 0.005 | 0.263 ± 0.005 |
| $E_{potential}$,[c] kcal/mol | −5.056 ± 0.000 | −4.800 ± 0.005 | 0.256 ± 0.005 |

[a] Averaged over the last five picoseconds of the simulations. [b] Change in energy/molecule after excitation. [c] Per molecule.

Instantaneous normal mode kinetic energies for the individual molecules as a function of time were computed using the recorded atomic properties and the projection method outlined in section II.C. Results for the excited molecules, unexcited molecules, and overall averages were averaged over the 12 trajectories at each recorded time step.

## III. Results and Discussion

The average final temperature of the NVE simulations is 306.1 K, which is an increase of about 12.6 K over the pre-excitation temperature. The overall kinetic energy introduced into the MD box through excitation of the 120 molecules corresponds to a temperature increase of 24.9 K for a classical system. Therefore, as expected, about half of the introduced kinetic energy was converted to potential energy. An end-point analysis of energies of the unexcited equilibrium liquid and the long-time state of the excited liquid was carried out. The motivation was to determine the distribution of the added energy among the various modes of the equilibrated liquid. These energies and pressure were averaged over the last five picoseconds of the 12 simulations. The results are shown in Table 2. The 0.519 kcal/mol per molecule difference in the total energies of the two liquids is equal to the expected difference because of the addition of 249.05 kcal/mol of energy to the total system.

Ensemble-averaged temperatures and the kinetic energies in the various normal modes were monitored for the duration of the simulations. As discussed in section II.D, a total of 249.05 kcal/mol was introduced to the system in the form of vibrational kinetic energy through equipartitioning of this energy into the CH stretching modes for 120 molecules in the system. Full equilibration of the system would result in half of this energy being transferred to potential energy. Additionally, the remaining kinetic energy should be equipartitioned among the translational, rotational, and vibrational degrees of freedom of the molecules in the system. The final temperature of a fully equilibrated system should be 305.9 K, 12.4 K above the initial temperature of the liquid.

The redistribution of the kinetic and potential energy of the system is seen in the time histories of the ensemble-averaged temperatures of excited and unexcited molecules (Figure 1a). At the beginning of NVE simulations, the temperature of the excited molecules is ∼100 K higher than that of the unexcited molecules. The figure shows that the excited molecules rapidly cool as the unexcited molecules become hotter. The cooling of the excited molecules can be represented by a single exponential with a decay constant of 13.0 ± 1.0 ps (95% confidence intervals quoted throughout). The heating of the unexcited molecules is described by a single exponential with rise constant of 10.1 ± 1.4 ps. The temperature of all molecules in the liquid reach the asymptotic limit expected for full equilibration shortly after 40 ps. The temperatures of the excited and unexcited molecules

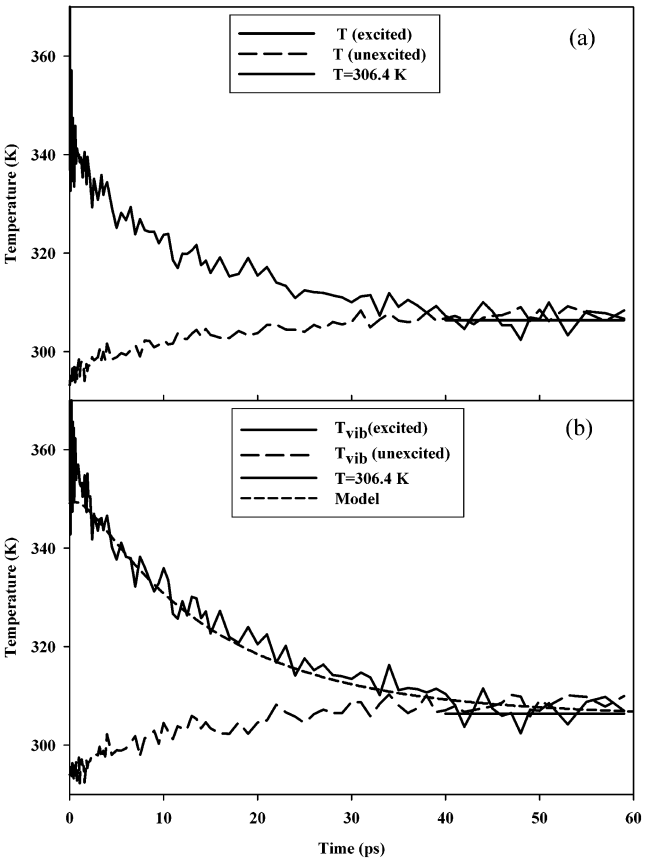


**Figure 1.** (a) Temperatures of excited (solid curve) and unexcited (long-dashed curve) nitromethane molecules, averaged over 12 NVE trajectories. (b) Vibrational temperatures (within the normal mode approximation) of excited (solid curve) and unexcited (long-dashed curve) nitromethane molecules, averaged over 12 NVE trajectories. The solid horizontal line from 40 to 60 ps in both frames denotes the expected temperature at the limit of full equilibration. The short-dashed curve in Figure 1b depicts predictions of the vibrational temperature of the system using eq 2. Errors in the averaged instantaneous temperatures of the excited molecules are as large as 25 K for the first 1 ps of the simulations; the magnitudes of the errors continually decrease in time, with error not exceeding 6 K beyond 7 ps. Errors in the instantaneous temperatures of the unexcited molecules are uniform throughout the simulations and do not exceed 3 K.

averaged over the time interval 40−60 ps are 306.7 ± 2.1 and 307.3 ± 1.1 K, in reasonable agreement with the expected value (305.9 K).

The equipartitioning of the energy among the molecular vibrational degrees of freedom using the kinetic normal mode energies can be seen in Figure 1b. Like the temperature curves shown in Figure 1a, the heating and cooling of the excited and unexcited molecules in the system are described by exponential functions with decay and rise constants of 14.6 ± 1.0 and 8.4 ± 1.5 ps, respectively. Also, the vibrational temperatures determined using normal mode kinetic energies are near the expected thermal equilibrium after 40 ps; vibrational temperatures averaged over the time interval 40−60 ps are 307.3 ± 2.4 and 308.4 ± 1.4 K for the excited and unexcited molecules.

Figures 2 and 3 show the time evolution of kinetic energies for the various normal modes of excited and unexcited molecules, respectively. Separate time histories were not recorded for degenerate mode pairs ($\nu_1$ and $\nu_2$, $\nu_5$ and $\nu_6$) or pairs of modes that represented rocking or wagging motions ($\nu_9$ and $\nu_{10}$, $\nu_{13}$ and $\nu_{14}$). Instead the time histories for these pairs were averaged and the resulting time histories are illustrated in frames (a), (c), (f), and (i), respectively, in Figures 2 and 3. The initial energy per mode before excitation of the asymmetric and symmetric $CH_3$ stretches is approximately 0.292 kcal/mol. Full equilibration of the system after excitation should result in an increase to 0.304 kcal/mol per vibrational mode (shown as the horizontal line in each frame of Figures 2 and 3). All normal mode energies of the excited molecules exhibit initial increases to some peak values before a gradual decline at longer times. In all cases the energies approach the expected equilibrium values within the time range 40−60 ps. The energies of the unexcited molecules increase gradually to the expected equilibrium values at the higher temperature.

Each curve in Figure 2 has been fitted to

$$\langle \mathrm{KE}_i \rangle = a_i \exp(-b_i t) + c_i \exp(-d_i t) + K \qquad (1)$$

where $i$ denotes the normal mode vibration and the constant $K$ is the asymptotic limit of energy expected upon full equilibration of the system (0.304 kcal/mol). This function was chosen to allow a description of the excitation of the normal mode and its subsequent energy loss as equilibration occurs. Predictions using eq 1 and best fit parameters to each curve in Figure 2 are superimposed on the corresponding time history curve in Figure 2. These curves can be used to identify the rise times and heights of the peak energies, as well as provide a guide for the eye. Peak heights and corresponding times are given in Table 3. Equation 1 can also be used to predict the overall vibrational temperature of the system. In this analysis, we assume the overall vibrational temperature of the system is

$$T(K) = \frac{2.0}{Mk} \sum_{i=1}^{M} \{a_i \exp(-b_i t) + c_i \exp(-d_i t) + K\} \qquad (2)$$

where $k$ is Boltzmann's constant and $M$ is the number of vibrational modes represented by eq 1. In this analysis, $M$ = 10, since the energy flow of the methyl group rotation was not followed (it is nearly a free rotor at the conditions of the simulation) and the energy flow of the $CH_3$ asymmetric stretches, the $CH_3$ asymmetric bends, the $CH_3$ rocks, and the $NO_2$ rocks are each represented by a single curve. A plot of eq 2 vs time is shown as the short-dashed line in Figure 1b; agreement with the simulation data for the excited molecules is quite good. A fit of this curve to a single exponential gives a decay constant of 14.7 ps, in good agreement with the decay constant obtained from fitting the vibrational temperature of the excited molecules in Figure 1b.

At the beginning of each NVE trajectory, each excited molecule has a total of 2.075 kcal/mol in the form of kinetic energy equally partitioned among the three CH stretching modes. If this energy was immediately redistributed equally among the vibrational degrees of freedom of the molecule, then the kinetic energy of vibration of each mode would increase from 0.292 to 0.341 kcal/mol. The information in Table 3 indicates that such an immediate and uniform redistribution does not occur. Immediate increases in kinetic energy in all vibrational modes upon relaxation of the C−H stretches is evident. However, the differences in the curves show that energy transfer into the modes occurs at different rates, indicating that VC occurs in stages. The decay of the C−H stretching vibrational modes is exponential; however, the $CH_3$ symmetric stretch ($\nu_3$) (Figure 2a) has a VER lifetime of 2.5 ps, whereas the $CH_3$ asymmetric stretching mode has a VER lifetime that is ∼3 times longer. The $CH_3$ asymmetric bends ($\nu_5$, $\nu_6$) (Figure 2c), $NO_2$ symmetric stretch ($\nu_8$) (Figure 2e), and $CH_3$ rocks ($\nu_9$, $\nu_{10}$) (Figure 2f) achieve their maximum level of excitation of ∼0.37−0.38 kcal/

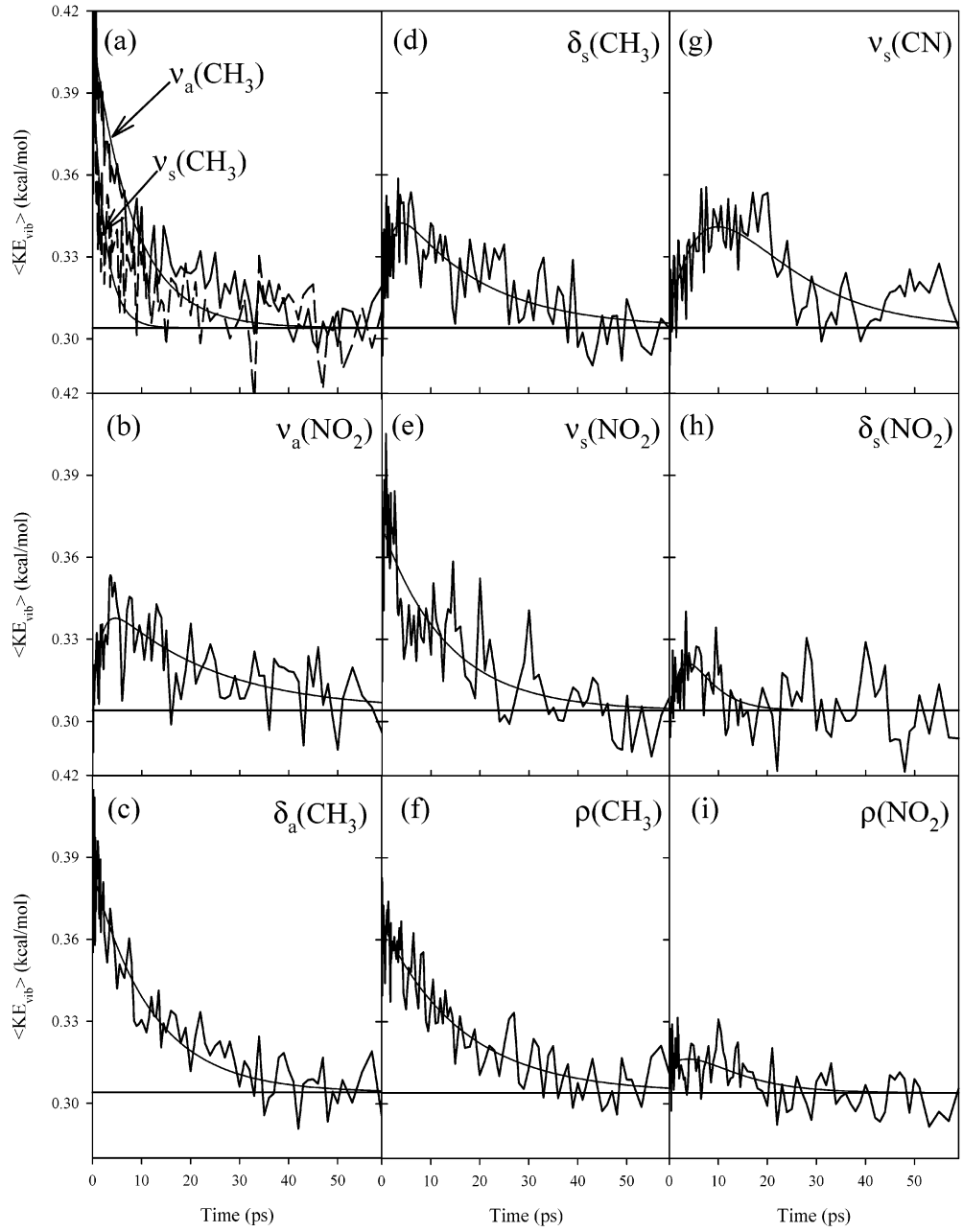


**Figure 2.** Average kinetic energies for normal modes (a) $\nu_1$, $\nu_2$, and $\nu_3$; (b) $\nu_4$; (c) $\nu_5$ and $\nu_6$; (d) $\nu_7$; (e) $\nu_8$; (f) $\nu_9$ and $\nu_{10}$; (g) $\nu_{11}$; (h) $\nu_{12}$; and (i) $\nu_{13}$ and $\nu_{14}$ of the excited nitromethane molecules. Solid curves in each frame depict fits of eq 1 to the data.

mol almost immediately. Energy flow from these vibrational modes occurs exponentially, with decay constants ranging from 11.9 to 16.2 ps. Four vibrational modes in the mid- to low-frequency range reach their maximum level of excitation at ~4 ps. The higher frequency $CH_3$ symmetric bend ($\nu_7$) (Figure 2d) and $NO_2$ asymmetric stretch ($\nu_4$) (Figure 2b) attain a maximum kinetic energy of 0.34 kcal/mol at 4 ps, and the lower frequency $NO_2$ symmetric bend ($\nu_{12}$) (Figure 2h) and rocking modes ($\nu_{13}$, $\nu_{14}$) (Figure 2i) attain a maximum energy of ~0.32 kcal/mol at 3.8 ps. Energy transfer from these modes can also be described as an exponential decay, but the lifetime of the low-frequency modes is much shorter than those of the higher frequency modes. Also, the temporal profile of the kinetic energy of the $NO_2$ symmetric bend ($\nu_{12}$) (Figure 2h) indicates that after the initial relaxation of this vibration, energy flows back into this mode at ~20 ps and appears to be localized for an additional 20 ps. The CN stretch mode ($\nu_{11}$) (Figure 2g) reaches its maximum excitation at 10 ps; energy flow from this point in time can be described as an exponential decay with lifetime ~20 ps. Although the kinetic energy appears to have reached the expected equilibrated value at 40 ps for this vibrational mode, energy flows back into the mode, suggesting that this mode remains excited and has not fully relaxed.

Figure 3 shows the kinetic energies for the vibrational modes for the unexcited molecules as functions of time. The profiles of the vibrational modes of the unexcited NM molecules (Figure 3) indicate that some VER from the excited NM to the bath occurs at the beginning of the VC process, though the degree of excitation is not great and the energy appears to be uniformly distributed among the vibrational modes. The behavior of the curves supports an indirect mechanism of IVET, characterized by Deak et al.[12] as a two-step process in which VC of the vibrationally hot NM excites the phonons in the liquid, which subsequently excite vibrations of the solvent molecules by multiphonon up-pumping. The main discrepancy between the Deak et al. results[12] and our results on the effect on the bath is

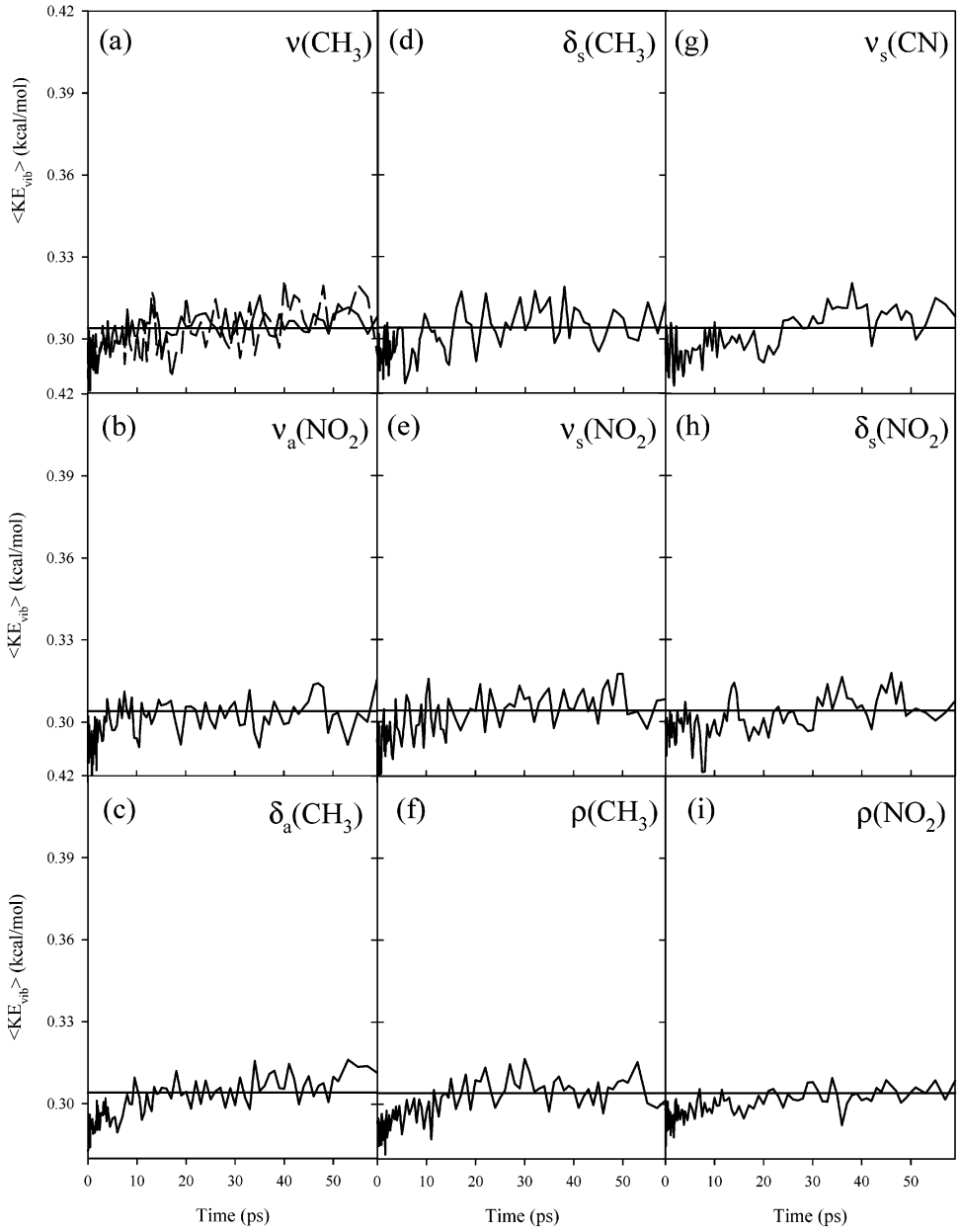


**Figure 3.** Same as Figure 2, except for the unexcited nitromethane molecules.

**TABLE 3: Best Fit Parameters of Curves in Figure 2 to Eq 1**

| mode | description | frequency, $cm^{-1}$ | decay constant,[a] ps | rise constant, ps | peak height, kcal/mol | time of max energy, ps | ⟨KE⟩[b] from 40 to 60 ps | |
|---|---|---|---|---|---|---|---|---|
| | | | | | | | excited | unexcited |
| $\nu_{1,2}$ | $\nu_a(CH_3)$ | 3095, 3093 | 8.2 | | 0.4120 | 0 | 0.305 ± 0.001 | 0.306 ± 0.001 |
| $\nu_3$ | $\nu_s(CH_3)$ | 2961 | 2.5 (2.6) | | 0.3972 | 0 | 0.306 ± 0.003 | 0.310 ± 0.002 |
| $\nu_4$ | $\nu_a(NO_2)$ | 1618 | 21.4 (15) | 1.7 | 0.3377 | 4.5 | 0.310 ± 0.003 | 0.305 ± 0.002 |
| $\nu_{5,6}$ | $\delta_a(CH_3)$ | 1436,1434 | 11.9 | | 0.3852 | 0 | 0.306 ± 0.002 | 0.308 ± 0.001 |
| $\nu_7$ | $\delta_s(CH_3)$ | 1508 | 17.0 (18) | 1.8 | 0.3423 | 4.0 | 0.301 ± 0.002 | 0.306 ± 0.002 |
| $\nu_8$ | $\nu_s(NO_2)$ | 1368 | 13.1 (18) | | 0.3714 | 0 | 0.303 ± 0.002 | 0.308 ± 0.002 |
| $\nu_{9,10}$ | $\rho(CH_3)$ | 1101, 1053 | 16.2 (30) | | 0.3666 | 0 | 0.307 ± 0.002 | 0.304 ± 0.001 |
| $\nu_{11}$ | $\nu_s(CN)$ | 821 | 12.5 (32) | 8.6 | 0.3410 | 10.0 | 0.315 ± 0.002 | 0.309 ± 0.001 |
| $\nu_{12}$ | $\delta_s(NO_2)$ | 605 | 4.4 (∼50) | 2.6 | 0.3214 | 3.8 | 0.303 ± 0.003 | 0.306 ± 0.001 |
| $\nu_{13,14}$ | $\rho(NO_2)$ | 601, 461 | 7.6 (∼50) | 6.1 | 0.3164 | 3.8 | 0.302 ± 0.002 | 0.304 ± 0.001 |

[a] Experimental decay constants from ref 12 are given in parentheses. [b] Average kinetic energy per mode averaged over excited and unexcited molecules. Units are in kcal/mol.

the time scale on which the heating of the bath occurs. In our simulations, we see heating beginning immediately. The Deak experiments monitored $CCl_4$ intensities to determine the onset of vibrational excitation in the solvent molecules. Their results showed that while some energy buildup in the bath occurs on the 15-ps time scale, the majority of heating occurs on the 50−100 ps time scale corresponding to the final step of VC.[12] At $t$ = 15 ps in our simulations, the temperature of the bath is within ∼20% of the expected equilibrium value, whereas at this time in the simulation, Deak et al.[12] estimate that only one-third of the total energy available has been dissipated to the unheated bath molecules, with the remainder being transferred to lower

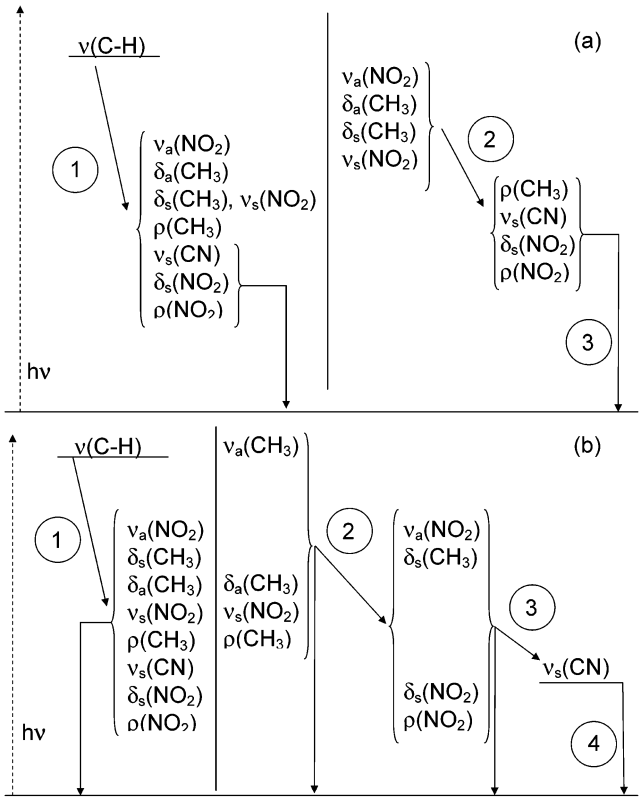


**Figure 4.** Energy level diagram showing stages of VER of nitromethane after C−H stretch excitation for (a) Deak et al. measurements (ref 12) and (b) this study.

frequency modes within the vibrationally hot molecules. It is possible that the differences between experiment and simulation in the time required for excitation of the bath molecules could be partially attributed to our use of unexcited NM molecules as the "molecular thermometers" to monitor the rise of bath excitation, rather than $CCl_4$ used in the Deak et al. study.[12]

The VC process of the excited NM molecules is illustrated in energy level diagrams showing stages of VER of NM after excitation of the C−H stretching vibrations (Figure 4). This figure is analogous to Figure 8 of Deak et al.,[12] in which the stages of VER in NM after C−H stretch excitation are presented. For convenience, we have included a depiction of the stages of VC in nitromethane observed by Deak et al.[12] (Figure 4a) and will discuss these before comparing with the simulation results (Figure 4b).

The results of the Deak et al. experiments show that VC of NM occurs through three stages.[12] In the first stage, the vibrationally excited C−H stretching vibrations relax, with their energy being deposited into the remaining vibrational modes of the molecule. The lifetime of the C−H stretching modes is 2.6 ps, consistent with the rise in populations observed for the vibrational modes of the molecule that were not excited by the pump pulse. The second stage of VC occurs through relaxation of the higher energy vibrations (1400 $cm^{-1}$ or greater). Lifetimes of these relaxations are on the order of ∼15 ps, which is consistent with the second of a two-part rise in populations of the low-energy vibrational modes (the faster part rises on the time scale of the C−H stretch decay). This indicates that the majority of excess energy in these vibrational modes is deposited into low-energy vibrations (there is evidence that there is some heating of the bath during this stage). The final stage of VC occurs through relaxation of the low-energy vibrations to the bath. VER lifetimes for these modes are on the order of 30−50 ps. Experimental results indicated that heating of the bath occurred on the same time scale as the final stage of the VC process.

In our study, the first stage of VC in the excited NM occurs through rapid relaxation of the excited C−H stretching vibrations, with all vibrational modes receiving some degree of excitation, in agreement with experiment. However, most of the energy from the C−H stretch decay is deposited in the symmetric $NO_2$ stretch, asymmetric $CH_3$ bend, and $CH_3$ rocking vibrations; these modes achieve the maximum level of excitation almost instantaneously. The lifetime of VER of the $CH_3$ symmetric stretch is 2.5 ps, in excellent agreement with the experimental results; however, the lifetime of VER in the $CH_3$ asymmetric stretching modes is approximately 3 times longer. This suggests that energy localized in the $CH_3$ symmetric stretch might be deposited into the $CH_3$ asymmetric stretch upon its relaxation. This was not observed in the experiment.

The second stage of VER in the simulation proceeds through decay of the $CH_3$ asymmetric stretch, symmetric $NO_2$ stretch, asymmetric $CH_3$ bend, and $CH_3$ rocking vibrations. The recipients of the energy from VER in this stage are the symmetric $CH_3$ and $NO_2$ bends, the asymmetric $NO_2$ stretch, and $NO_2$ rocking modes. While the experimental results indicated the low-energy vibrations ($<$1400 $cm^{-1}$) were populated by relaxation of higher energy vibrations ($>$1400 $cm^{-1}$), we cannot ascribe such a mechanism. The states that first relax consist of both high- and low-frequency modes, as do the vibrations that are subsequently excited. The third stage of VER proceeds through deposition of energy into the CN stretch before reaching the final stage of the VC process in which the excess energy is dissipated from the molecule to the bath. The lifetime of VER of the CN stretching mode (∼20 ps) is much shorter than the experimental lifetimes of the low-frequency modes from which energy is dissipated to the bath (30−50 ps).

Overall, the features of the VER and VC processes in liquid NM resulting from our simulation are in qualitative agreement with experiment: (1) Vibrational energy initially deposited in the CH stretching modes rapidly flows into all vibrations of the molecules. (2) The vibrational modes excited by the VER of the CH stretches relax at different rates, resulting in a VC mechanism that occurs in stages. (3) The final stage of vibrational cooling is the dissipation of the excess energy to the bath. (4) Vibrational modes of the unexcited NM are excited predominantly through indirect IVET processes. Differences are seen in (1) the lifetimes of VER (particularly for the low-frequency modes), (2) the time required to achieve full equilibration of the system, and (3) details of the path of energy flow as energy is redistributed in the vibrational levels before dissipation to the bath. The discrepancies in the path of intramolecular energy flow and decay/excitation times between the model and experiments could be attributed to a number of factors. However, our feeling is that these discrepancies are due mainly to inadequacies in the potential energy function used in the study. The simple form describing intramolecular motions does not exactly reproduce the quantum mechanical information to which it was fitted. This is evident in the lack of agreement in vibrational frequencies, particularly for the vibrational mode corresponding to the $CH_3$ symmetric bend. Additionally, this model does not reproduce exactly the density of the liquid at the conditions of the experiment; the theoretical result is too small by ∼4%. These factors, along with limitations of the simulations due to the classical approximation, could easily affect the VC process.

## IV. Conclusions

Classical NEMD simulations have been performed to study vibrational energy transfer in liquid NM after excitation of the CH stretching vibrations. Results were compared with those of Deak et al.,[12] who used anti-Stokes Raman spectroscopy to directly monitor the VER and VC processes in liquid NM after infrared excitation in the C−H stretching region. The simulation results show qualitative agreements with the experimental data,[12] including a rapid relaxation of the excited CH stretches into different vibrational modes of the molecules, a multistage VC process, and excitation of modes of the surrounding unexcited molecules through indirect rather than direct IVET processes. However, because the results here were obtained using classical MD simulations, they do not reflect quantum effects that might influence the energy-transfer process. Therefore, future goals are directed toward quantum mechanical treatments starting with smaller and computationally manageable systems, with an expectation that computational advances will allow quantum treatments of larger systems.

**Acknowledgment.** This work was performed while V.N.K. held a National Research Council Senior Resident Research Associateship at the U.S. Army Research Laboratory. Some calculations reported in this work were performed at the Army Research Laboratory Major Shared Resource Center, Aberdeen Proving Ground, MD.

## References and Notes

(1) Tokmakoff, A.; Fayer, M. D.; Dlott, D. D. *J. Phys. Chem.* **1993**, *97*, 1901.
(2) Fried, L. E.; Ruggiero, A. J. *J. Phys. Chem.* **1994**, *98*, 9786.
(3) McNesby, K. L.; Coffey, C. S. *J. Phys. Chem. B* **1997**, *101*, 3097.
(4) Ye, S. J.; Tonokura, K.; Koshi, M. *Combust. Flame* **2003**, *132*, 240 .
(5) Tarver, C. M. *J. Phys. Chem. A* **1997**, *101*, 4845.
(6) Tas, G.; Franken, J.; Hambir, S. A.; Hare, D. E.; Dlott, D. D. *Phys. Rev. Lett.* **1997**, *78*, 4585.
(7) Holmes, W.; Francis, R. S.; Fayer, M. D. *J. Chem. Phys.* **1999**, *110*, 3576.
(8) Dlott, D. D.; Fayer, M. D. *J. Chem. Phys.* **1990**, *92*, 3798.
(9) Chen, S.; Tolbert, W. A.; Dlott, D. D. *J. Phys. Chem.* **1994**, *98*, 7759 .
(10) Chen, S.; Hong, X.; Hill, J. R.; Dlott, D. D. *J. Phys. Chem.* **1995**, *99*, 4525.
(11) Hong, X.; Chen, S.; Dlott, D. D. *J. Phys. Chem.* **1995**, *99*, 9102.
(12) Deak, J. C.; Iwaki, L. K.; Dlott, D. D. *J. Phys. Chem. A* **1999**, *103*, 971.
(13) Dlott, D. D. *Chem. Phys.* **2001**, *266*, 149.
(14) Dlott, D. D. *Accounts Chem. Res.* **2000**, *33*, 37.
(15) Dlott, D. D. *Annu. Rev. Phys. Chem.* **1999**, *50*, 251.
(16) Hu, W. F.; He, T. J.; Chen, D. M.; Liu, F. C. *J. Phys. Chem. A* **2002**, *106*, 7294.
(17) Nguyen, M. T.; Le, H. T.; Hajgató, B.; Veszprémi, T.; Lin, M. C. *J. Phys. Chem. A* **2003**, *107*, 4286.
(18) Manaa, M. R.; Fried, L. E. *J. Phys. Chem. A* **1998**, *102*, 9884.
(19) Saxon, R. P.; Yoshimine, M. *Can. J. Chem.* **1992**, *70*, 572.
(20) McKee, M. L. *J. Phys. Chem.* **1989**, *93*, 7365.
(21) McKee, M. L. *J. Am. Chem. Soc.* **1986**, *108*, 5784.
(22) McKee, M. L. *J. Am. Chem. Soc.* **1985**, *107*, 1900.
(23) Kaufman, J. J.; Hariharan, P. C.; Chabalowski, C.; Hotokka, M. *Int. J. Quantum Chem.* **1985**, *Suppl. 19*, 221−235.
(24) Cook, M. D.; Haskins, P. J. Proceedings of the 9th Symposium (International) on Detonation, Portland, OR, 1989; p 1027.
(25) Cook, M. D.; Fellows, J.; Haskins, P. J. In *"Decomposition, Combustion and Detonation Chemistry of Energetic Materials"*; Brill, T. B., Russell, T. P., Tao, W. C., Wardles, R. B., Eds.; *Materials Research Society Symposium Proceedings 418*; Materials Research Society: Pittsburgh, PA, 1996; p 267.
(26) Margetis, D.; Kaxiras, E.; Elstner, M.; Frauenhem, T.; Manaa, M. R. *J. Chem. Phys.* **2002**, *117*, 788.
(27) Rice, B. M.; Thompson, D. L. *J. Chem. Phys.* **1990**, *93*, 7986.
(28) Soulard, L. In *Shock Compression of Condensed Matter*; Furnish, M. D., Thadani, N. N., Horie, Y., Eds.; AIP: Woodbury, NY, 2001; p 173.
(29) Soulard, L, AIP Conference Proceedings 2002; 620; Shock Compression of Condensed Matter, Part 1; p 347.
(30) Decker, S. A.; Woo, T. K.; Wei, D.; Zhang, F. *Proceedings of the 12th International Detonation Symposium (International)*; San Diego, CA; 2003.
(31) Tuckerman, M. E.; Ungar, P. J.; VonRosenvinge, T.; Klein, M. L. *J. Phys. Chem.* **1996**, *100*, 12878.
(32) Tuckerman, M. E.; Klein, M. L. *Chem. Phys. Lett.* **1998**, *283*, 147.
(33) Alper, H. E.; AbuAwward, F.; Politzer, P. *J. Phys. Chem. B* **1999**, *103*, 9738.
(34) Seminario, J. M.; Concha, M. C.; Politzer, P. *Int. J. Quantum Chem.* **1995**, (*S29*), 621.
(35) Seminario, J. M.; Concha, M. C.; Politzer, P. *J. Chem. Phys.* **1995**, *102*, 8281.
(36) Sorescu, D. C.; Rice, B. M.; Thompson, D. L. *J. Phys. Chem. B* **2000**, *104*, 8406.
(37) Sorescu, D. C.; Rice, B. M.; Thompson, D. L. *J. Phys. Chem. A* **2001**, *105*, 9336.
(38) Agrawal, P. M.; Rice, B. M.; Thompson, D. L. *J. Chem. Phys.* **2003**, *119*, 9617.
(39) Reed, E. J.; Joannopoulos, J. D.; Fried, L. E. *Phys. Rev. B* **2000**, *62*, 16 500.
(40) Oxtoby, D. W. *Annu. Rev. Phys. Chem.* **1981**, *32*, 77.
(41) Owrutsky, J. C.; Raftery, D.; Hochstrasser, R. M. *Annu. Rev. Phys. Chem.* **1994**, *45*, 519.
(42) Miller, D. W.; Adelman, S. A. *Int. Rev. Phys. Chem.* **1994**, *13*, 359.
(43) Egorov, S. A.; Skinner, J. L. *J. Chem. Phys.* **1996**, *105*, 7047.
(44) Rey, R.; Hynes, J. T. *J. Chem. Phys.* **1996**, *104*, 2356.
(45) Everitt, K. F.; Egorov, S. A.; Skinner, J. L. *Chem. Phys.* **1998**, *235*, 115.
(46) Sibert, E. L.; Rey, R. *J. Chem. Phys.* **2002**, *116*, 237.
(47) Everitt, K. F.; Skinner, J. L.; Ladanyi, B. M. *J. Chem. Phys.* **2002**, *116*, 179.
(48) Lawrence, C. P.; Skinner, J. L. *J. Chem. Phys.* **2002**, *117*, 5827.
(49) Lawrence, C. P.; Skinner, J. L. *J. Chem. Phys.* **2003**, *119*, 1623.
(50) Shi, Q.; Geva, E. *J. Chem. Phys.* **2003**, *118*, 7562.
(51) Terashima, T.; Shiga, M. *J. Chem. Phys.* **2001**, *114*, 5663.
(52) Shiga, M.; Okazak, S. *J. Chem. Phys.* **1999**, *111*, 53990; **2000**, *113*, 6451.
(53) Mikami, T.; Okazak, S. *J. Chem. Phys.* **2003**, *119*, 4790.
(54) Mikami, T.; Shiga, M.; Okazaki, S. *J. Chem. Phys.* **2001**, *115*, 9797.
(55) Voth, G. A. *Adv. Chem. Phys.* **1996**, *93*, 135.
(56) Jang, S.; Pak, Y.; Voth, G. A. *J. Phys. Chem. A* **1999**, *103*, 10289.
(57) Käb, G. *Phys. Rev. E* **2002**, *66*, 046 117.
(58) Whitnell, R. M.; Wilson, K. R.; Hynes, J. T. *J. Phys. Chem.* **1990**, *94*, 8625.
(59) Whitnell, R. M.; Wilson, K. R.; Hynes, J. T. *J. Chem. Phys.* **1990**, *96*, 5354.
(60) Brown, J. K.; Harris, C. B.; Tully, J. C. *J. Chem. Phys.* **1988**, *89*, 6687.
(61) Vikhrenko, V. S.; Heidelbach, C.; Schwarzer, D.; Nemtsov, V. B.; Schroeder, J. *J. Chem. Phys.* **1999**, *110*, 5273.
(62) Heidelbach, C.; Vikhrenko, V. S.; Schwarzer, D.; Schroeder, J. *J. Chem. Phys.* **1999**, *110*, 5286.
(63) Heidelbach, C.; Fedchenia, I.; Schwarzer, D.; Schroeder, J. *J. Chem. Phys.* **1998**, *108*, 10152.
(64) Heidelbach, C.; Schroeder, J.; Schwarzer, D.; Vikhrenko, V. S. *Chem. Phys. Lett.* **1998**, *291*, 333.
(65) Chorny, I.; Vieceli, J.; Benjamin, I. *J. Chem. Phys.* **2002**, *116*, 8904.
(66) Neufeld, A. A.; Schwarzer, D.; Schroeder, J.; Troe, J. *J. Chem. Phys.* **2003**, *119*, 2502.
(67) Figueirido, F. E.; Levy, R. M. *J. Chem. Phys.* **1992**, *97*, 703.
(68) Egorov, S. A.; Berne, B. J. *J. Chem. Phys.* **1997**, *107*, 6050.
(69) Raff, L. M. *J. Chem. Phys.* **1988**, *89*, 5680.
(70) Raff, L. M. *J. Chem. Phys.* **1989**, *90*, 6313.
(71) Sorescu, D. C.; Thompson, D. L.; Raff, L. M. *J. Chem. Phys.* **1994**, *101*, 3729.
(72) Pan, R.; Raff, L. M. *J. Phys. Chem.* **1996**, *100*, 8085.
(73) Rahaman, A.; Raff, L. M. *J. Phys. Chem. A* **2001**, *105*, 2147.
(74) Chen, S.; Lee, I.-Y. S.; Tolbert, W. A.; Wen, X.; Dlott, D. D. *J. Phys. Chem.* **1992**, *96*, 7178.
(75) Kim, H.; Dlott, D. D. *J. Chem. Phys.* **1991**, *94*, 8203.
(76) Smith, W.; Forester, T. R. *DLPOLY2 Simulation Package*, *version 2.13*, CCLRC, Daresbury Laboratory, Daresbury, Warrington, England, 1996.
(77) Allen, M. P.; Tildesley, D. J. *Computer Simulation of Liquids*; Clarenden Press: Oxford, 1987.
(78) Berendsen, H. J. C.; Postma, J. P. M.; van Gunsteren, W.; DiNola, A.; Haak, J. R. *J. Chem. Phys.* **1984**, *81*, 3684.
(79) Melchionna, S.; Ciccotti, G.; Holian, B. L. *Mol. Phys.* **1993**, *78*, 533.
(80) Rabinovich, I. B. *Influence of Isotopy on the Physico-Chemical Properties of Liquids*; Consultants Bureau: New York, 1970.